

MRS Photodiode, LED and Extruded Scintillator Performance in Magnetic Field

D. Beznosko, G. Blazey, A. Dyshkant, V. Rykalin, V. Zutshi

Abstract—The experimental results on the performance of the MRS (Metal/Resistor/Semiconductor) photodiode in the strong magnetic field of 4.4T, and the possible impact of the quench of the magnet at 4.5T on sensor's operation are reported. In addition, the experimental results on the performance of the extruded scintillator and WLS fiber, and various LEDs in the magnetic fields of 1.8T and 2.3T respectively, are detailed. The measurement method used is being described.

I. INTRODUCTION

Future detectors (like Digital Hadron Calorimeter [1] [2] for a future e^+e^- linear collider) may require the use of scintillator cells with embedded photodetectors, immersed in a strong magnetic field. This imposes constraints on the performance of the photodetectors, scintillators and LEDs for calibration system use. The photodetector performance requirement has directed our attention to the latest developments in the field of solid-state photomultipliers working in avalanche mode [3].

However, it is not always obvious how to measure various properties of scintillator, fibers, LEDs and photodetectors in the strong field's presence. Firstly, in this paper we have concentrated on the possible issues of the MRS output in the presence of strong magnetic field; i.e., the dependence of output's amplitude, area and rise time on the field, and the effects of magnet's quench on the sensor. Also, an accent was placed on the method of measuring the scintillator response to UV LED light in the presence of magnetic field, i.e., the dependence of output's amplitude and area on the field was studied. In addition, the performance of various LEDs in the magnetic field was measured as well.

II. DESCRIPTIONS AND SCHEMATICS

A. MRS Photodiode Description and Operational Principle

The MRS photodiode is a multi-pixel solid-state device with every pixel operating in the limited Geiger multiplication mode. A resistive layer on the sensor surface achieves avalanche

quenching. The devices tested were of round shape, and they had ~ 1000 pixels per 1.1mm diameter photosensitive area, with the quantum efficiency (QE) of the device reaching over $\sim 25\%$ at 500nm [4]. Due to the fact that the thickness of the active layer of this sensor is about 7 microns, theoretically MRS is expected to be non-sensitive to the magnetic field.

B. Magnet Description - MRS

All magnetic field measurements were performed at the Fermilab Magnet Test Facility. The magnet used for MRS measurements only was a standard Tevatron Dipole [5], whose field strength was ~ 1 Tesla per kA. The sensors were placed in the body of the magnet (far from the ends), where the field is very uniform (at the level of 1 part in 10000). The dipole field direction is vertical. The temperature in the magnet aperture is not cryogenic and is close to "room" temperature. The following characterizes the speed with which magnetic field collapses during a quench event: the current in the magnet decays (approximately) exponentially with a time constant of about 0.25 seconds (determined by the L/R of the circuit that are not adjustable).

C. Magnet Description – LED and Scintillator

A GMW Helmholtz Dipole Magnet, model 3474, by GMW Associates [6], was used for LED and scintillator measurements only. The diameter of the poles is 250mm, with maximum current of 140 Amps at 76 Volts (10.6kW) while water-cooled. The field strength is dependent on the distance between the poles. Due to this limitation, the highest field achieved was 2.3T.

D. LED List

The following LEDs were measured:

1. Bivar [7] LED5-UV-400-30 T1 3/4 5mm UV LED with peak emission at 400nm;
2. Lumex [8] SSL-DSP5093USBC Ultra Blue with peak emission at 475nm, and SSL-LX5093UPGC/C Ultra Pure Green with peak emission at 525 nm;
3. Radioshack [9] 276-351 T-1-3/4 (5mm) Yellow LED with peak emission at 587nm, 276-320 5mm White LED with peak emission not listed, and 276-041 5mm Red LED with peak emission at 700nm.

Manuscript received May 14, 2005. This work was supported in part by the U.S. Department of Education under Grant No. P116Z010035, the Department of Energy, and the State of Illinois Higher Education Cooperation Act.

D. Beznosko, G. Blazey, A. Dyshkant, K. Francis, D. Kubik, V. Rykalin, V. Zutshi are with Northern Illinois University, DeKalb, IL 60115 USA (telephone: 815-753-3504, email: dyshkant@fnal.gov).

E. MRS Module Description

For this test, five MRS sensors were used, arranged in different directions with respect to the magnetic field. All sensors were biased at 30.0V that was well within operating range of all five. An optical splitter was used to deliver similar light pulse to each of the sensors.

The crystal used for splitting the light had a square cross-section being 5mm wide and 30mm long. At the output (front) end it had five symmetrical conical holes with 2mm base diameter for each of them (Fig. 1a). The conical surfaces were not polished. Without these conical holes, the ratio of the direct light along the crystal to the “side” light at the front end the crystal was about 10 to 1. With the conical holes, this ratio was less than two. No further effort was made to achieve the same amount of light in all directions since the goal was to get a comparable amount of light only. The positions of the photodetectors around the crystal were determined by these holes. The light splitting property of the crystal as measured by the same sensor is presented in Fig. 1b. Table I shows the various properties of MRS output for all 5 sensors in their places for the test signal in the absence of magnetic field.

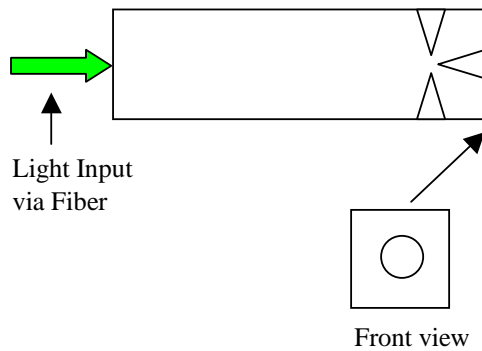


Fig. 1a. Schematic of the splitting crystal.

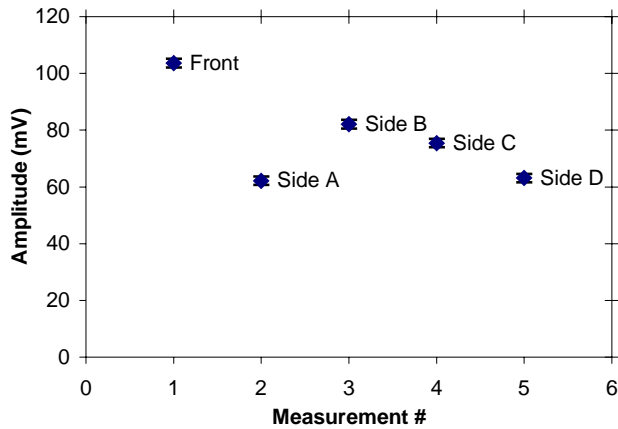


Fig. 1b. Uniformity of light output of splitting crystal.

TABLE I
OUTPUTS FOR 5 CHANNELS WITH TEST SIGNAL

Channel #	1	2	3	4	5
Area (nVs)	15.24	23.12	10.75	25.59	13.51
Amptd (mV)	38.79	45.86	27.18	50.6	38.31
Rise time (ns)	30.55	43.16	33.69	38.94	30.50

The light pulse was produced by the Bivar [7] UV LED (peak emission ~400nm). The pulse from the pulse generator was ~30ns wide with ~5.5V amplitude. The LED was embedded into the 10mm thick extruded scintillator [10]. The LED-scintillator part was placed well outside the magnet to avoid any effects of the field since only the photodetectors were studied here. The light pulse from the scintillator to the splitter was carried via ~2.5m long, 2mm outer diameter, KURARAY [11], multicladd, Y-11, wavelength shifting (WLS) fiber. The output of the sensors was fed into the Agilent [12] Infinium 54832D MSO oscilloscope without additional preamplifier. The schematic of this module is given in Fig. 2a, and the schematic of the power circuit for the MRS is drawn in Fig. 2b. The temperature inside the magnet was measured before and after the tests and was $5.8^{\circ}\text{C} \pm 0.5$.

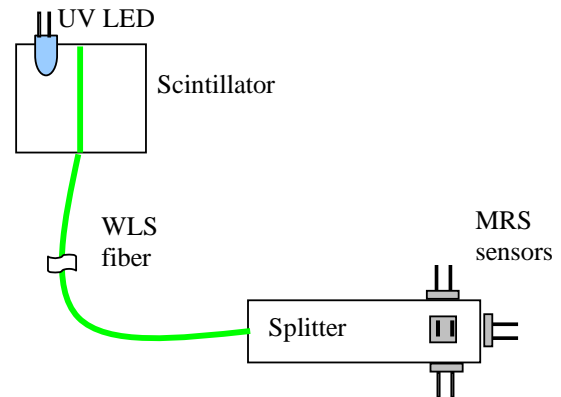


Fig. 2a. MRS module schematics.

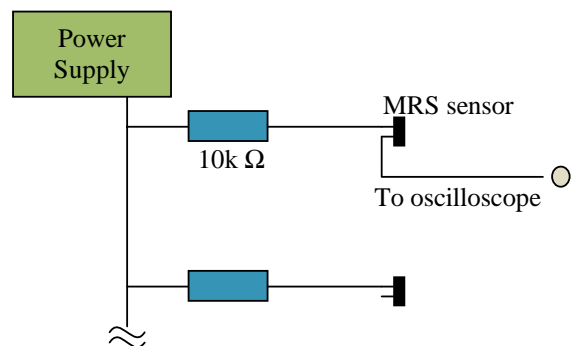


Fig. 2b. MRS power circuit schematics.

F. LED Module Description

For this test, MRS sensor was used, arranged such that the light from the LED was incident directly onto the photosensitive area via small aperture. The sensor was biased at 30.0V that is well within its operating range.

Fig. 3a shows the photograph of the module, Fig. 3b shows its schematic and Fig. 3c is the detailed module photograph.

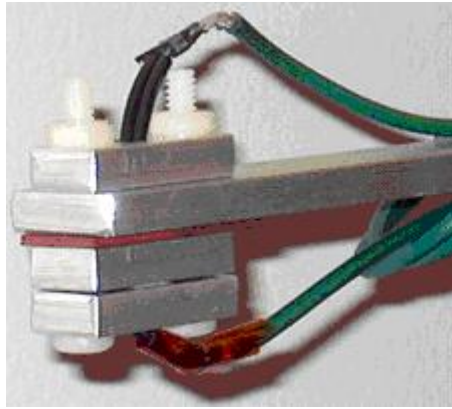


Fig. 3a. LED module.

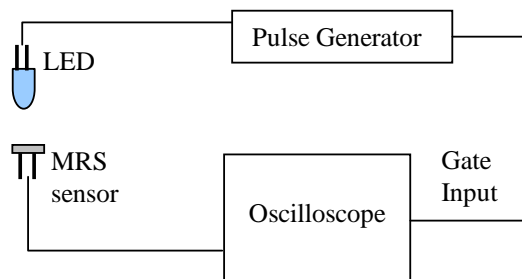


Fig. 3b. LED module schematic.

The light pulse was produced by the easily changeable LED. The pulse from the pulse generator was ~30ns wide. Different amplitudes for various LEDs were needed. The output of the MRS sensor was measured and recorded by Agilent [12] Infiniium 54832D MSO oscilloscope without additional preamplifier. The module was placed between the poles of the magnet in a fashion similar to shown in Fig. 4c.

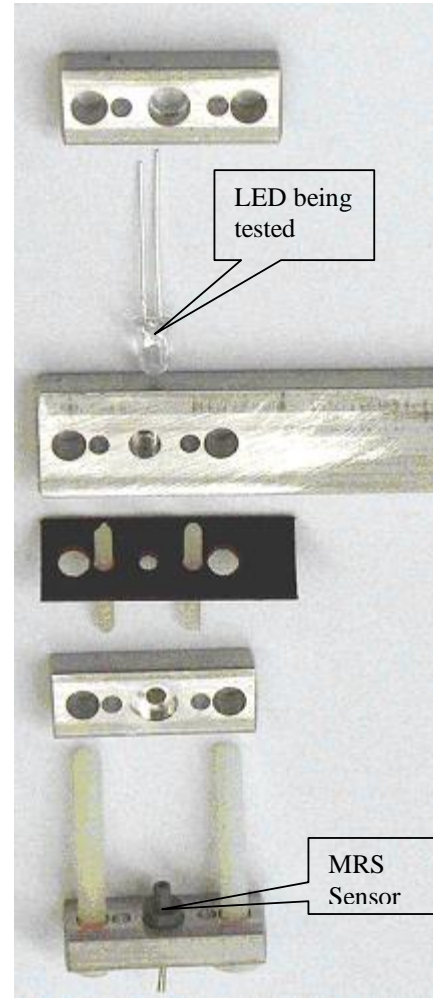


Fig. 3c. LED module in details.

G. Scintillator Module Description

For this test, 10cm x 2cm x 1cm extruded [10] scintillator bar covered by reflective material was used. The KURARAY [11] multiclad Y-11 1mm outer diameter WLS fiber was inserted into the co-extruded hole, also Bivar [7] UV LED and the MRS sensor were used, arranged such that the light from the LED was incident directly onto the scintillator only. This way, the WLS fiber would pick up the light only from the scintillator itself and not from the UV LED. The MRS sensor was placed in contact with the free end of the fiber, and was biased at 30.0V that is well within its operating range.

Fig. 4a shows the photograph of the module with WLS fiber not inserted. Note that the fiber terminal position was above the LED and is indicated by the red line on the figure. Fig. 4b shows the schematic of the module. Fig. 4c shows the module between the magnet poles.

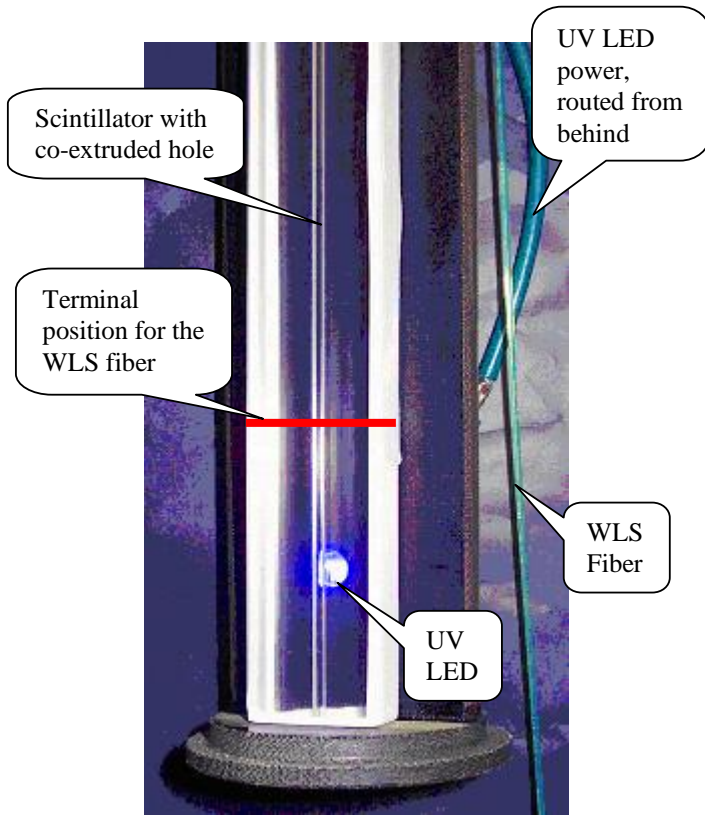


Fig. 4a. Scintillator module. Red line indicates the terminal position of the WLS fiber when inserted, so that it doesn't pick up light directly from the UV LED.

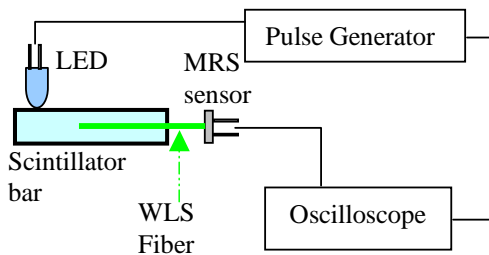


Fig. 4b. Scintillator module schematic.

The pulse to the LED from the pulse generator was ~ 30 ns wide. The output of the MRS sensors was measured and recorded by Agilent [12] Infiniium54832D MSO oscilloscope without additional preamplifier.

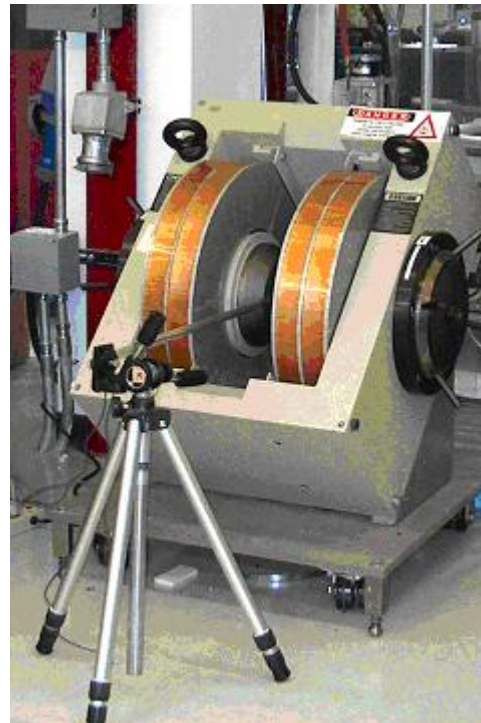


Fig. 4c. Scintillator Module between the magnet poles.

III. EXPERIMENTAL SECTION

A. MRS Experimental Results

The data for all 5 channels were obtained. Because of the similarity of the results, data only for channel 4 will be presented for illustrative purposes (data for other channels is in the Appendix). This channel corresponds to the MRS sensor that was positioned at the tip of the splitter. The electrons in this sensor move along the same axis inside the dipole as the particle beam would, therefore, the MRS in channel 4 should experience the biggest effects of the B field, if any.

The following characteristics of the sensor's output were measured: amplitude, area, and rise time. Measurements were carried out at 0T, 4.0066T, 0T, 4.0065T, 0T and 4.4077T. The repeated measurements at 0T were conducted in order to eliminate unknown factors like the possible temperature changes during the experiment. In addition, measurements were conducted immediately after magnet quench at 4.5T (the field was zero during these measurements). The pole with the sensors and the LED-scintillator module was inserted into the magnet approximately 12 hours before the experiment so that it would be at the same temperature as inside the dipole. A constant stream of nitrogen was pumped through the magnet throughout the test to remove the humidity.

Fig. 5 is the superposition of the MRS output of channel 4 at 0T, 4T, 4.4T, and after quench at 4.5T. The scale here is 20mV per cell on vertical axis and 200ns per cell on horizontal.

From Fig. 5 there are no immediate indications of differences in the output that could be easily seen by the eye. Fig. 6 shows the values of the area of MRS output as a function of the magnetic field strength. The area is a measure of total charge of the output with a 50Ω load. Each point in every figure is an average of at least few hundred measurements at each field strength value. The errors are given directly by the oscilloscope. Here and in all further plots 4.5qT label indicates a measurement done after the magnet quench at 4.5T field. The q-l and q-l-m labeled data points were taken at 0T some time (approximately 5 and 10 minutes) after the experiment, with the oscilloscope, power supply and signal generator being turned off and back on between q-l and q-l-m measurements. The biggest difference between points at 0T and 4T is $\sim 1.5\%$ that is within the measurement error. However, all the points at 4T seem to differ from the 0T ones, whereas all the point measured at 0T have much smaller spread. Other channels do not show this systematic difference of output values.

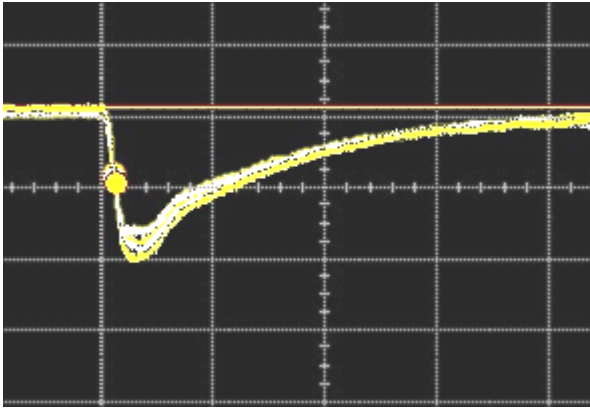


Fig. 5. Superposition of the MRS outputs at the field strengths of 0T, 4T, 4.4T, and after quench at 4.5 T. The scale is 20mV per cell on vertical axis and 200ns per cell on horizontal one.

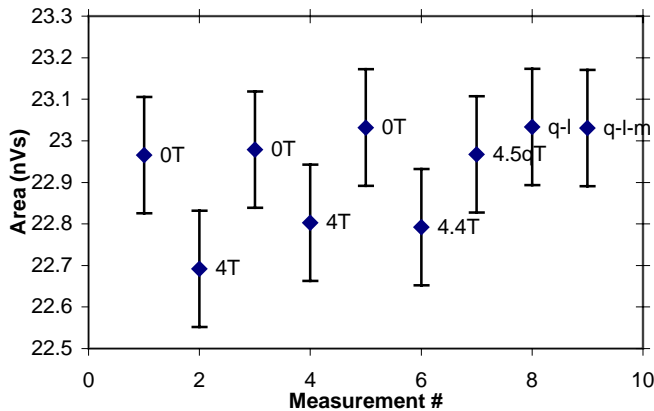


Fig. 6. Area of the MRS output.

Fig. 7 shows the values of the amplitude of MRS output as a function of the magnetic field strength. The amplitude is a measure of the peak current of the output with a 50Ω load. The maximum of $\sim 1\%$ change in output amplitude between field strength values 0T and 4.4T is observed.

The dependence of rise time on the magnetic field strength was also studied (Fig. 8). The behavior of the signal rise time seems to be quite independent on the field strength; however, this could be due to the fact that the spread of the values is smaller than the jitter introduced by the way oscilloscope measures the rise time.

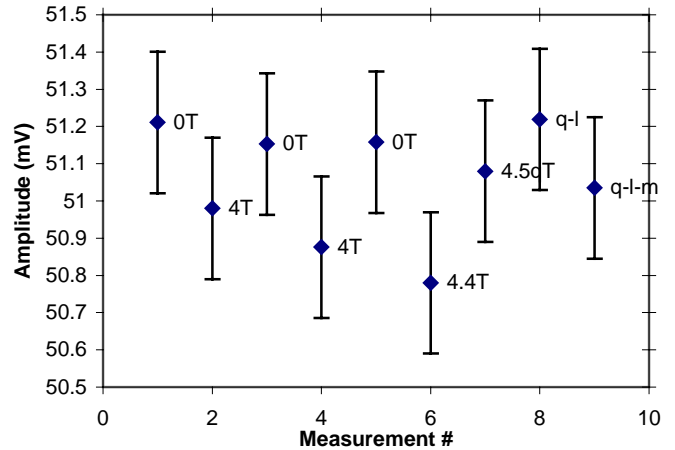


Fig. 7. Amplitude of the MRS output.

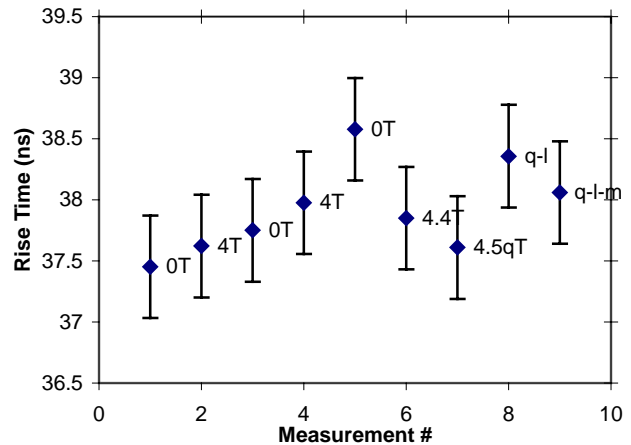


Fig. 8. Rise time of the MRS output.

The performed tests using 5 MRS sensors in the 4.4T magnetic field indicate the insensitivity of the sensor's output on the field strength within $\sim 1\%$. This result enables us to use MRS to measure the LED and scintillator responses in the magnetic field.

B. LED Experimental Results

The data for all LEDs listed in section C was obtained. Because of the similarity of the results, data only for Bivar UV LED will be presented for illustrative purposes. Bivar LED is of special interest since it doesn't change the spectral characteristics of its light output with change in current [13].

Here, the field is perpendicular to the LED. The amplitude and the area of the output were measured. Measurements were carried out at 0T, maximum field, 0T, maximum field again, 0T, etc. The repeated measurements at 0T are conducted in order to eliminate unknown factors like the possible temperature or time changes during the experiment. In addition, the field was increased and decreased as fast as possible. Fig. 9 is the superposition of the MRS output for Bivar UV LED at 0T and successive measurement at 2.3T. The full output amplitude is ~124mV in both measurements, with area ~ 4.7nVs.

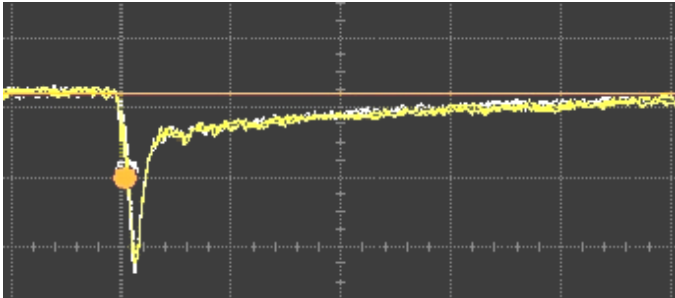


Fig. 9. Superposition of the outputs at the field strengths of 0T (white) and 2.3T (yellow). The scale is 50mV per cell on vertical axis and 50ns per cell on horizontal.

From Fig. 9 there are no immediate indications of differences in the output that could be easily seen by the eye. Fig. 10 shows the values of the area of MRS output for Bivar UV LED different magnetic field strengths.

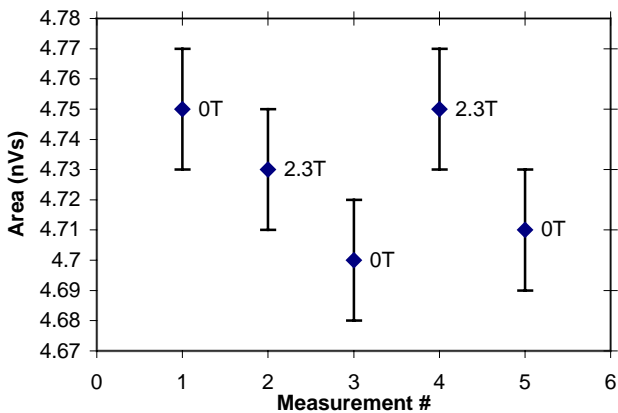


Fig. 10. Area of the MRS output for Bivar UV LED.

The area is a measure of total charge of the output with a 50Ω load that is dependent on the total amount of incident light. Each point is an average of at least few hundred measurements. The errors are given directly by the oscilloscope. The biggest difference between points at 0T and 2.3T is ~1% that is within the measurement error.

Fig. 11 shows the values of the amplitude of MRS output for Bivar UV LED at different magnetic field strengths. The amplitude is a measure of the peak current of the output with a 50Ω load that is dependent on the peak light output from the LED. The maximum of ~1% change in output amplitude between field strength values 0T and 2.3T is observed.

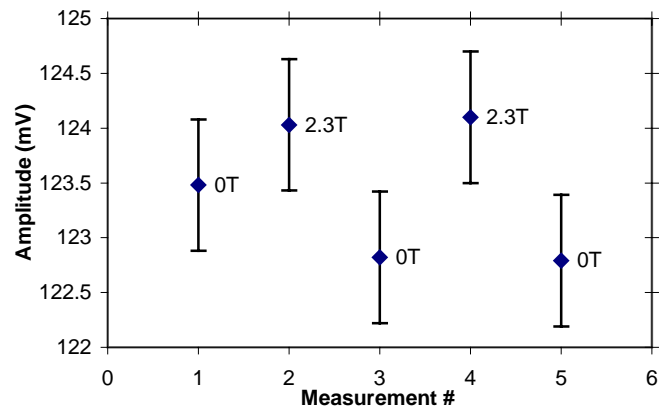


Fig. 11. Amplitude of the MRS output for Bivar UV LED.

Similar results are observed for the field being parallel to the UV LED (here, due to module dimensions (Fig. 3a), the maximum achievable field was 1.8T). Analogous results (Table II) are observed for Lumex and Radioshack LEDs in the perpendicular field (2.3T) as well. Note that sometimes the maximum value of output will be at 0T and sometimes at 2.3T.

TABLE II
LED RESPONSE CHANGE IN THE MAGNETIC FIELD

LED TESTED	CHANGE IN OUTPUT (%)	COLOR
SSL-DSP5093USBC	1.4	Blue Superbright
SSL-LX5093UPGC/C	0.7	Green Suberbright
276-351 T-1-3/4	1.6	Yellow Bright
276-320 T-1-3/4	1.5	White Bright
276-041 T-1-3/4	1.2	Red Regular

In addition, the dependence of LED light output on temperature was conducted using the Bivar [7] UV LED with constant amplitude pulses (not current pulses). For this measurement, a setup similar to one in Fig. 3b was used. The differences were that a Hamamatsu [14] R-580 Photomultiplier (PMT) was used, and LED and the PMT were at some distance from each other, aligned in a way such that the LED would shine directly upon the photosensitive area of the PMT. The PMT was biased at 900V for increased stability. The LED was placed on the heating element with temperature being monitored at the LED itself. At each measurement point, few minutes were given for temperature inside LED to stabilize. The result of this measurement is shown in Fig. 12. Note that here a source of constant amplitude pulse was used to power LED, and not a more commonly used current course.

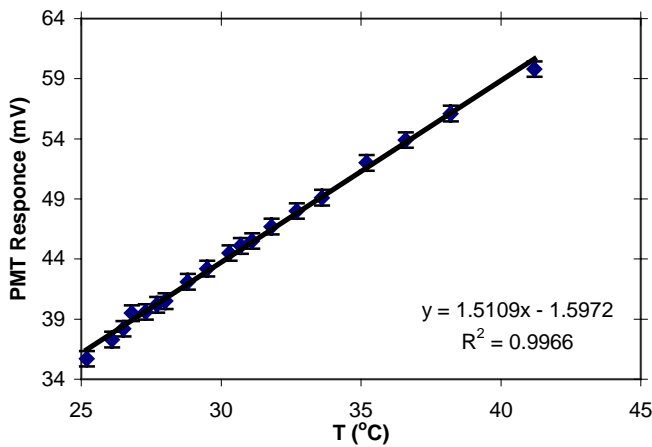


Fig. 12. Light output of the UV LED as measured by the PMT vs. temperature.

C. Extruded Scintillator Experimental Results

With UV LED and the MRS photosensor both being insensitive of the magnetic field presence, one can carry out the measurements for the scintillator in the B field. Even though the thorough measurements of various scintillators were done earlier [15], we have carried out the measurements for the newly available and not yet tested in the B field extruded scintillator [10] with the Kuraray [11] Y11 1mm diameter WLS fiber embedded in the co-extruded hole.

Here, the field is parallel to the LED (i.e. perpendicular to the fiber). The amplitude and the area of the output were measured. Measurements again were carried out at 0T, maximum field, 0T, maximum field again, 0T, etc. The repeated measurements at 0T were conducted in order to eliminate unknown factors like the possible temperature changes during the experiment, since no thermometer was used to check the temperature. Time was given for temperature to stabilize inside the module (~20 minutes), but some temperature shift is still unavoidable, in part due to the fact that

the temperature of magnet and water cooling is not constant while working. Fig. 13 is the superposition of the MRS output for extruded scintillator at 0T and successive measurement at 1.8T. The full output amplitude here is ~129mV in both measurements, with area ~ 8.4nVs.

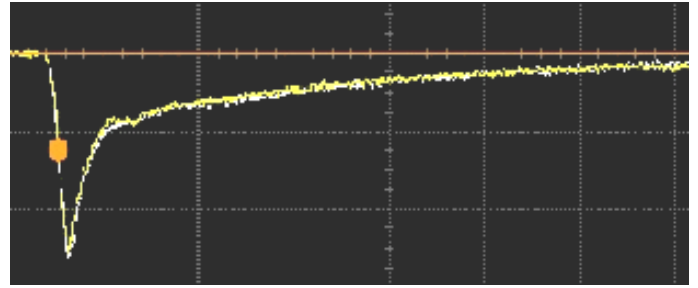


Fig. 13. Superposition of the outputs at the field strengths of 0T (white) and 1.8T (yellow). The scale is 50mV per cell on vertical axis and 50ns per cell on horizontal. Due to technical reasons not all the cells might be visible.

From Fig. 13 there are no immediate indications of differences in the output that could be easily seen by the eye. Fig. 14 shows the values of the area of MRS output for extruded scintillator at different magnetic field strengths.

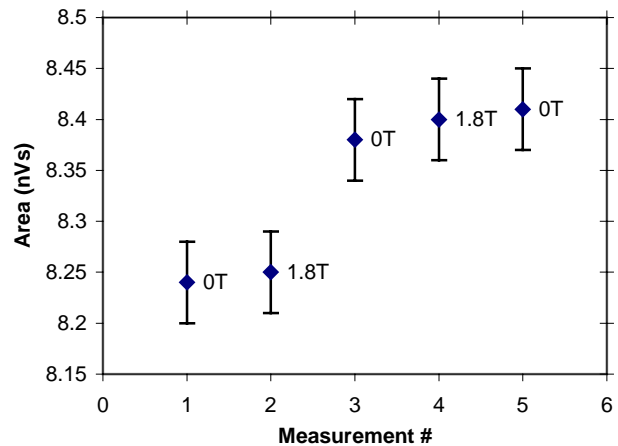


Fig. 14. Area of the MRS output for extruded scintillator.

The area is a measure of total charge of the output with a 50Ω load that is dependent on the total amount of incident light that depends on any changes in scintillator properties. Each point in every figure is an average of at least few hundred measurements at each field strength value. The errors are given directly by the oscilloscope. The biggest difference between points at 0T and 1.8T is <1% counting in the fact that between first two point and the remaining three the temperature of the module was changed as indicated by the measurements taken at 0T, and the difference due to the magnetic field should be calculated using points from each group only.

Fig. 15 shows the values of the amplitude of MRS output for extruded scintillator at different magnetic field strengths. The

amplitude is a measure of the peak current of the output with a 50Ω load that is dependent on the peak light output from the scintillator. The maximum of $<1\%$ change in output amplitude between field strength values 0T and 1.8T is observed. Once again, the temperature of the module was changed between first two points and the remaining three measurements and difference should be calculated using points from each group.

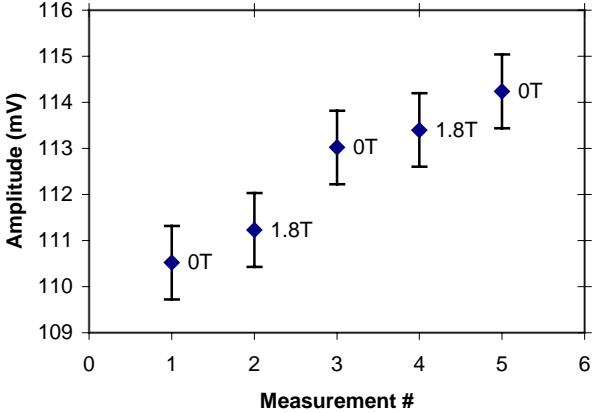


Fig.15. Amplitude of the MRS output for extruded scintillator.

IV. CONCLUSIONS

Measurements performed using 5 MRS sensors in the strong magnetic field point to the insensitivity of the sensor’s output on the field strength of up to 4.4T within 1%-1.5%. There are also indications that magnet quench has none or immeasurably small effect on the sensors. However, a small but quite systematic difference of the output values at 0T and 4T for channel 4 (other channels do not show this pattern) may warrant further investigation of this topic, possibly with higher fields strength values.

Measurements performed using various LEDs in the magnetic field point to the insensitivity of the LED’s light output on the field strength of up to 2.3T within 1%. This result allows using UV LED in conjunction with MRS sensors to measure the properties of the extruded scintillator in the magnetic field. The results of this measurement indicate the insensitivity of the light output levels of extruded scintillator to the magnetic fields up to 1.8T within 1% when excited by the UV LED.

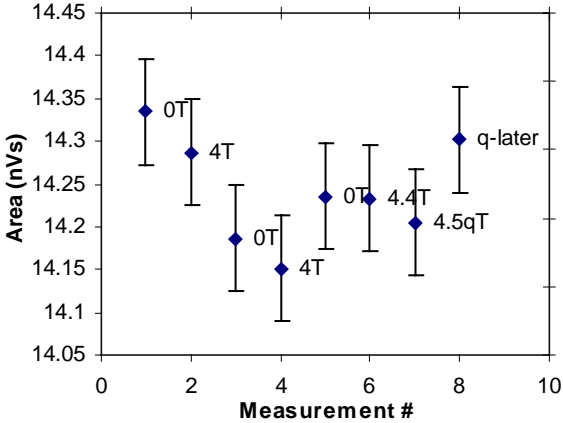


Fig. 16. Area of the MRS output for channel #1.

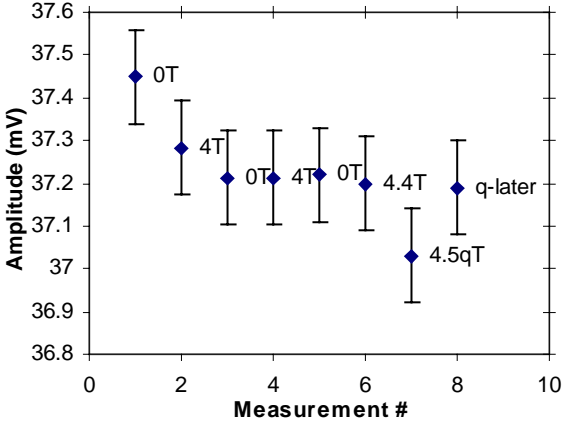


Fig. 17. Amplitude of the MRS output for channel #1.

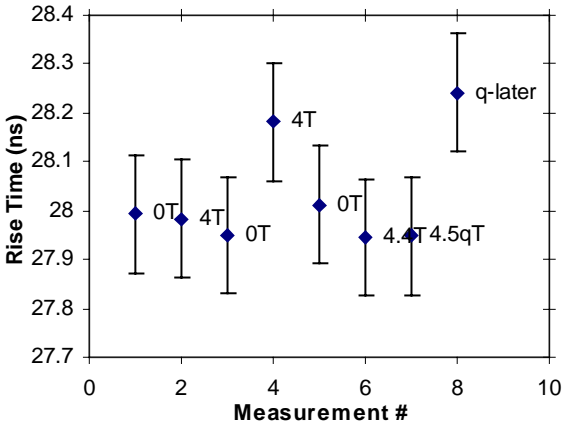


Fig. 18. Rise time of the MRS output for channel #1.

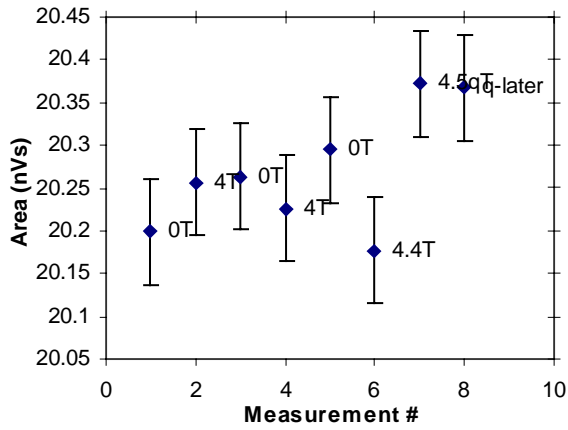


Fig. 19. Area of the MRS output for channel #2.

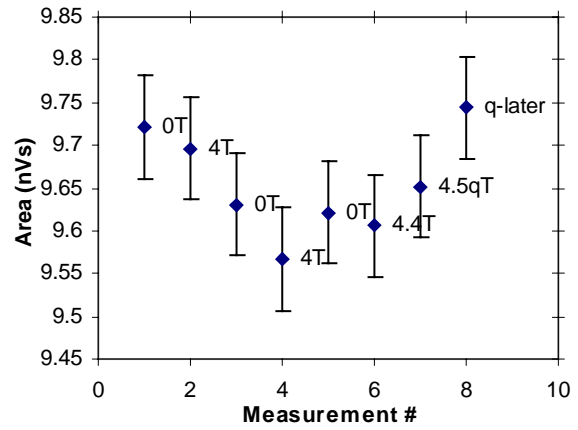


Fig. 22. Area of the MRS output for channel #3.

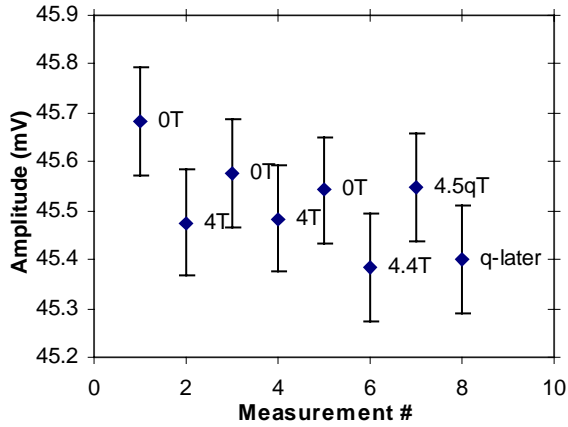


Fig. 20. Amplitude of the MRS output for channel #2.

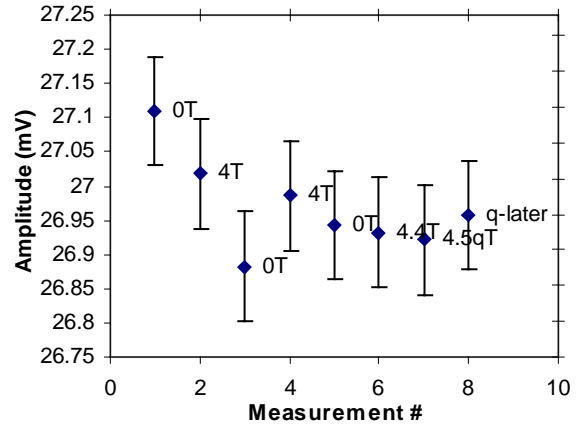


Fig. 23. Amplitude of the MRS output for channel #3.

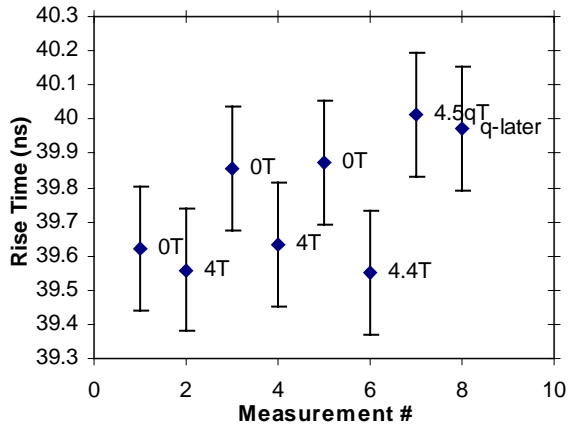


Fig. 21. Rise time of the MRS output for channel #2.

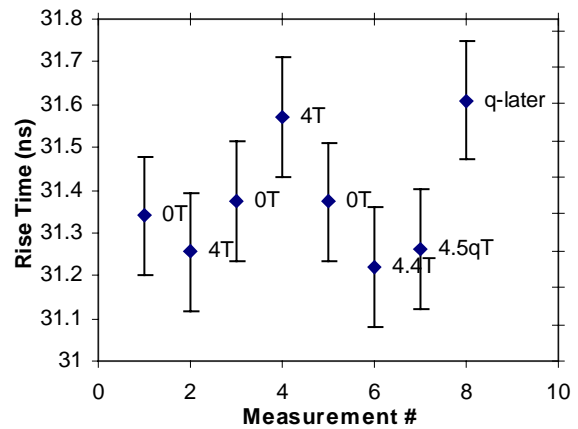


Fig. 24. Rise time of the MRS output for channel #3.

ACKNOWLEDGMENT

The authors would like to thank Michael Tartaglia for permitting the use of the Fermilab Magnet Test Facility, Boris Baldine for useful advice, and Pat Richards, Larry Gregersen and Phillip Stone for providing excellent mechanical and machining support.

REFERENCES

- [1] A. Dyshkant, D. Beznosko, G. Blazey, D. Chakraborty, K. Francis, D. Kubik et al., "Towards a Scintillator-Based Digital Hadron Calorimeter for the Linear Collider Detector", IEEE vol. 51, no. 4, pp.1590-1595, Aug. 2004.
- [2] A. Dyshkant, D. Beznosko, G. Blazey, D. Chakraborty, K. Frances, D. Kubik et al, "Small Scintillating Cells as the Active Elements in a Digital Hadron Calorimeter for the e+e- Linear Collider Detector", FERMILAB-PUB-04/015, Feb 9, 2004
- [3] D. Beznosko, G. Blazey, A. Dyshkant, K. Francis, D. Kubik, A. Pla-Dalmau et al., "MRS Photodiode", FERMILAB-CONF-04-210-E, September 15, 04
- [4] M. Golovin, A.V. Akindinov, E.A. Grigorev, A.N. Martemyanov, P.A. Polozov, "New Results on MRS APDS", Nucl. Instrum. Meth. A387 231-234, 1997
- [5] R. Hanft, B. C. Brown, W. E. Cooper, D. A. Gross, L. Michelotti, E. E. Schmidt et al., "Magnetic Field Properties of Fermilab Energy Saver Dipoles", FERMILAB-TM-1182, March 1983
- [6] GMW Associates, 955 Industrial Road, San Carlos, CA 94070
- [7] Bivar Inc., 4 Thomas, Irvine, CA 92618, USA
- [8] Lumex, Inc., 290 East Helen Road Palatine, IL 60067, USA.
- [9] RadioShack Corporation, Riverfront Campus World Headquarters, 300 RadioShack Circle, Fort Worth, TX 76102-1964, USA.
- [10] D. Beznosko, A. Bross, A. Dyshkant, A. Pla-Dalmau V. Rykalin, "FNAL-NICADD Extruded Scintillator", FERMILAB-CONF-04-216-E, September 15, 04
- [11] Kuraray America Inc., 200 Park Ave, NY 10166,USA; 3-1-6, NIHONBASHI, CHUO-KU, TOKYO 103-8254, JAPAN.
- [12] Agilent Technologies, Inc. Headquarters, 395 Page Mill Rd., Palo Alto, CA 94306, United States
- [13] P. Adamson, J. Alner, B. Anderson, T. Chase, P.J. Dervan, T. Durkin et al., "The MINOS light-injection calibration system," NuMI-PUB-SCINT, FD_DOCS-0743, NIM A 492 (2002) 325-343, Oct. 21, 2002.
- [14] Hamamatsu Corporation, 360 Foothill Road, PO Box 6910, Bridgewater, NJ 08807-0919, USA; 314-5,Shimokanzo, Toyooka-village, Iwata-gun, Shizuoka-ken, 438-0193 Japan.
- [15] Dan Green, Anatoly Ronzhin, Vasken Hagopian, "Magnetic Fields and Scintillator Performance", FERMILAB-TM-1937, June 1995.

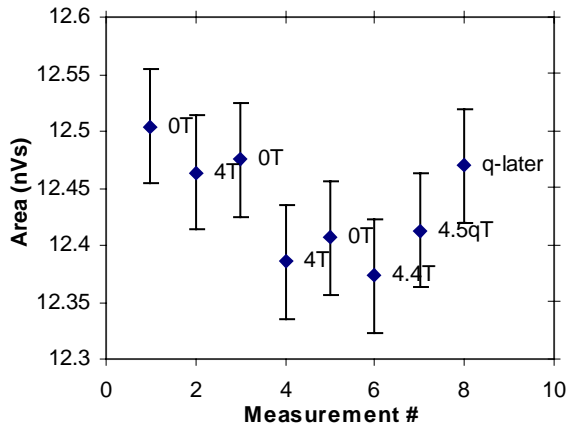


Fig. 25. Area of the MRS output for channel #5.

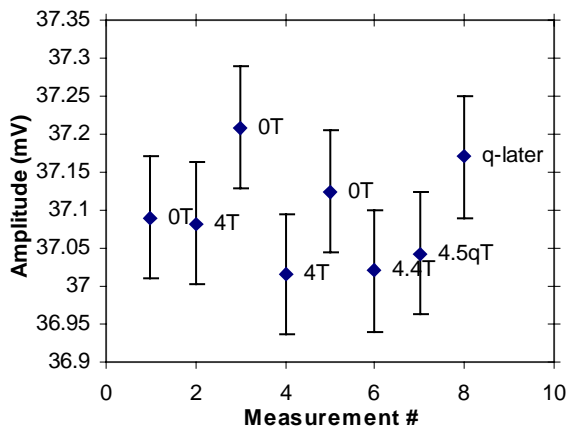


Fig. 26. Amplitude of the MRS output for channel #5.

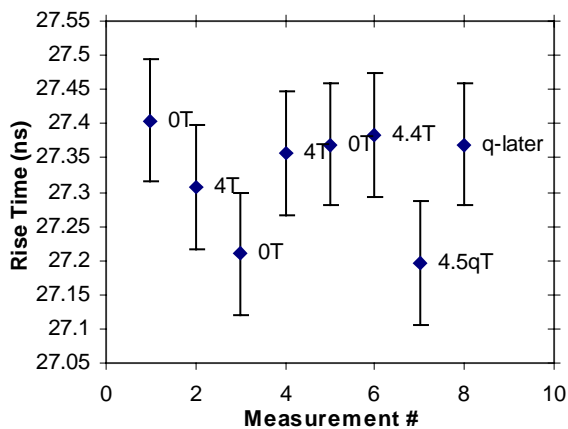


Fig. 27. Rise time of the MRS output for channel #5.